Conformation and Orientation of Tetraalanine in a Lyotropic Liquid Crystal Studied by Nuclear Magnetic Resonance

Silvia Pizzanelli, Susanna Monti, and Claudia Forte*

Istituto per i Processi Chimico-Fisici, Consiglio Nazionale delle Ricerche, Area della Ricerca di Pisa, via G. Moruzzi 1, 56124 Pisa, Italy

Received: April 7, 2005; In Final Form: August 8, 2005

The ^{1}H NMR spectra of two isotopomers of tetraalanine deuterated on the two external methyl groups and on the two internal ones, respectively, were recorded in the lyotropic solvent cesium pentadecafluorooctanoate (CsPFO)/water. Eight dipolar couplings could be estimated from the spectra. The set of dipolar couplings was fitted assuming that one rigid conformer is present. Of the four major conformers considered, selected on the basis of theoretical calculations, the one characterized by the two couples of internal dihedral angles in the Ramachandran region of PPII resulted to be the only one to fit the set of couplings within experimental error. The data indicate that the molecule is oriented with the long molecular axis tilted with respect to the surface of the micelles formed by CsPFO.

1. Introduction

Alanine-based model peptides have been extensively studied by experimental means with the aim of obtaining conformational information. It was long believed that in short peptides each residue can exist in all conformations assignable to the sterically allowed region in the Ramachandran plot,[1,2] which are considered nearly isoenergetic. However, most recent studies have led to a modification of this view and ample evidence was provided that these oligopeptides can adopt a limited number of conformers in solution.

The collection of experimental observations on peptide systems is important not only to test the accuracy of the computational findings but also to suggest possible refinements to the theoretical models for a correct description of the systems under examination.

Theoretical studies of the conformational dynamics of oligopeptides are generally performed using methods based on all-atom protein force fields due to the prohibitively large computational time needed by ab initio calculations in order to achieve reasonable conformational sampling. Unfortunately, the methods based on force fields have often shown defects in reproducing the measured conformational distributions of peptide molecules. However, comparisons with experiments have allowed the introduction of simple modifications in the force fields to extend their applicability and to reproduce measured data.[3]

According to several studies, alanine residues can adopt a polyproline II helix (PPII) conformation in water. The frequent occurrence of PPII backbone conformation in relatively long peptides and denatured proteins is strongly supported by early circular dichroism (CD) studies[4−10] together with investigations by vibrational CD,[11] Raman optical activity,[12] and NMR.[13] Structural studies on very short alanine peptides have also been reported. For example, both experimental[14−16] and theoretical[17] evidence for the dominance of PPII in alanine dipeptide in water was collected in several studies. Tri- and tetraalanine in aqueous solution in different protonation states were investigated by means of a variety of techniques (two-dimensional vibrational spectroscopy,[18,19] Raman, IR, and CD spectroscopies,[20,21] and polarized Raman, Fourier transform IR, and vibrational CD techniques[22]). The results of these studies suggested that trialanine adopts only the PPII conformation or, alternatively, that two conformers with PPII and β-strand-like structure coexist in aqueous solution, while tetraalanine adopts only the PPII conformation. For a review on PPII as a major backbone conformation in unfolded proteins see ref 23. In this work, we use liquid-crystal NMR spectroscopy to investigate the conformation and orientation of tetraalanine in a lyotropic phase. Our aim was to compare our conformational results with those already reported for the same molecule in water,[22] thus testing the dependence of the conformation on the environment. In fact, the interaction of aqueous dissolved tetraalanine with the hydrophobic species of the lyomesophase might induce conformational changes with respect to the pure water phase. Moreover, our results on the orientation of the molecule might be helpful in elucidating the factors influencing the interaction of oligopeptides with the hydrophobic species of this type of mesophases.

Liquid-crystal NMR spectroscopy has been used to investigate the structure as well as the orientation of rigid and flexible solutes in an anisotropic environment.[24,25] The liquid crystal orients in the external magnetic field exhibiting dipolar couplings but also induces partial orientational order on the solute so that dipolar couplings are also observed for molecules dissolved in the anisotropic medium, yielding information on molecular geometry. The liquid crystal used in the present work is the lyotropic system cesium pentadecafluorooctanoate (CsPFO)/water. CsPFO forms bilayer-like disk-shaped micelles near pH 7 in water,[26] which makes this liquid crystal a good candidate for mimicking biomembrane systems. In fact, the conformation and orientation of various biologically active molecules have been investigated using this mesophase.[27,28] In addition, this system offers the practical advantage of being devoid of protons, so that the proton signal of the solute can be observed without dynamic range problems.

Since the spectrum of fully protonated tetraalanine in the anisotropic phase is rather complex because of extensive signal

* Corresponding author. E-mail address: c.forte@ipcf.cnr.it.

10.1021/jp051797p CCC: $30.25 © 2005 American Chemical Society
Published on Web 10/14/2005

overlap, the approach we used to simplify the spectra was to substitute some of the protons with deuterium nuclei. In particular, we estimated the four different intra-methyl and the four intraresidue methyl−methine values of proton dipolar couplings from the combination of measurements on two tetraalanine samples, one deuterated on the two external methyl groups (isotopomer **I**) and the other deuterated on the two internal ones (isotopomer **II**). Since the dipolar couplings depend on geometry and orientational order, defined by five independent order parameters, the set of eight dipolar couplings could be fitted assuming that only one rigid conformer is present. Four major conformers, obtained through theoretical calculations in solution, were tested.

2. Experimental Section

Ala-3,3,3-d_3−Ala-Ala-Ala-3,3,3-d_3 (trifluoroacetate salt) (**I**) and Ala-Ala-3,3,3-d_3−Ala-3,3,3-d_3−Ala (trifluoroacetate salt) (**II**) were prepared according to a procedure reported in the literature.[29] The degree of deuteration was 99% on the basis of the purity of the starting materials used in the synthesis of **I** and **II**. CsPFO was prepared according to a procedure reported in the literature.[15]

NMR samples were prepared by weighing CsPFO directly into an NMR tube and adding 40 wt % D_2O (Aldrich, 99.9%) with a syringe. With the composition used, an isotropic−nematic N_D^+ phase transition is expected to occur at about 309 K, the range of stability of the nematic phase being approximately 10 K. Homogeneous solutions were obtained simply by heating the samples to the isotropic phase and shaking. **I** or **II** was dissolved in the CsPFO/D_2O solution at a concentration of 0.2−0.3 wt %. The pH of the samples was approximately 7; at this pH, tetraalanine is zwitterionic.

All the NMR experiments were carried out on a Bruker AMX-300 WB, equipped with a 5 mm reverse probe. The $\pi/2$ pulses were 12 and 10.5 μs on the ^1H and ^2H channel, respectively. The sample temperature was controlled by a BVT 1000 (Eurotherm) variable-temperature unit, with a temperature stability of ±0.1 K.

^1H single pulse experiments were carried out in the temperature range 313−292 K, with and without ^2H decoupling during the acquisition, using the GARP sequence for decoupling with a suitable decoupler power in order to have efficient decoupling but minimum sample heating. The relaxation delay was set to 5 s.

Two-dimensional (2D) J-resolved experiments were performed on I in the isotropic and in the anisotropic phase using a standard Bruker pulse program to which a 4 s presaturation pulse (B1 = 25 Hz) was added in order to reduce the water signal. The 2D spectrum was taken with 8192 data points in F2 and with 128 increments in F1, using 16 scans for each FID and a recycling delay of 4 s. The spectral width on F1 was set to 40 Hz and to 1200 Hz for the sample in the isotropic and anisotropic phase, respectively.

^2H single pulse experiments were carried out in the temperature range 313−292 K, with a relaxation delay of 4 s, to check the degree of order in the mesophase from the D_2O quadrupolar splitting.

The dipolar couplings were estimated from the anisotropic ^1H spectra employing the program SpinWorks written and made available by Dr. Kirk Marat.[30] The fitting of the estimated dipolar couplings was performed using a home-written program within the Mathematica 5 environment.[31] The order parameters were optimized using a multiparameter nonlinear least-squares optimization routine based on the Levenberg−Marquardt algorithm. The dipolar couplings between all the couples of protons in each isotopomer were calculated from the order parameters and the geometry using a home-written program within the Mathematica 5 environment.[31]

3. Theoretical Background

The dipolar coupling between two nuclei i and j in a liquid crystalline medium can be expressed as[32]

$$D_{ij} = -K_{ij}\langle 1/r_{ij}^3\rangle[S_{zz}\cos^2\theta_z^{ij} + S_{yy}\cos^2\theta_y^{ij} + (-S_{zz} - S_{yy})\cos^2\theta_x^{ij} + 2\cos\theta_z^{ij}\cos\theta_x^{ij}S_{zx} + 2\cos\theta_z^{ij}\cos\theta_y^{ij}S_{zy} + 2\cos\theta_x^{ij}\cos\theta_y^{ij}S_{xy}] \quad (1)$$

where $K_{ij} = (\gamma_i\gamma_j/4\pi^2)h$, r_{ij} is the internuclear distance, θ_α^{ij} ($\alpha = x, y, z$) is the angle between the internuclear vector and the axis x, y, or z of an arbitrary molecular frame, respectively, and $S_{\alpha\beta}$ ($\alpha, \beta = x, y, z$) are the elements of the Maier−Saupe order matrix with respect to the direction of the external magnetic field Z, defined as $S_{\alpha\beta} = (1/2)\langle 3\cos\theta_\alpha^Z\cos\theta_\beta^Z - \delta_{\alpha\beta}\rangle$. The angular brackets indicate an average over all molecular motions, i.e., internal rotations, vibrations and overall reorientation. Equation 1 is valid only if reorientation is slow compared to the internal motions.

The order matrix, which describes the orientational distribution of the molecular fixed frame in space, is a symmetric and traceless tensor and therefore is generally defined by five independent elements. The axes system (x', y', z') in which the order matrix is diagonal, i.e., the order principal axes system (PAS), is usually chosen with z' the axis of maximum orientation. The estimation of five or more direct couplings for a given rigid conformer allows the five elements of its order matrix to be determined and therefore also the order matrix in the PAS and the orientation of the PAS with respect to a molecular fixed frame. If N conformers are simultaneously present, 5N experimental constraints are required to determine the order matrix of each one, an additional variable being their relative populations. In the present work, given the experimental data available, we would have to make arbitrary assumptions on the order of each conformer and on their population. Thus, also considering the observations from IR, Raman, and vibrational circular dichroism on cationic tetraalanine,[22] we assumed that only one conformer is present.

We assumed that vibrational averaging is mimicked well by a single effective geometry and used eq 1 replacing $\langle 1/r_{ij}^3\rangle$ with the inverse of the cube of the internuclear distance in the best-fit geometry derived according to the procedure outlined in the following paragraph.

4. Results and Discussion

4.1. Conformers Selection and Optimization by Means of Theoretical Calculations. To calculate the dipolar couplings D_{ij}, related to the molecular geometry through eq 1, we selected four conformers on the basis of a previous study where molecular dynamics simulations with CHARMM24 all-atom force field were used.[33]

Each conformer is defined by the nine dihedral angles shown in Figure 1, ψ_i ($i = 1-3$), φ_j and ω_j ($j = 2-4$), the subscript indicating, as usual, the residue. The most populated conformers of tetraalanine are characterized by the internal torsional angles (φ_2,ψ_2) and (φ_3,ψ_3) belonging to the Ramachandran region of stability of PPII or α helix conformations.[33] The four possible combinations of these conformations for the two couples of

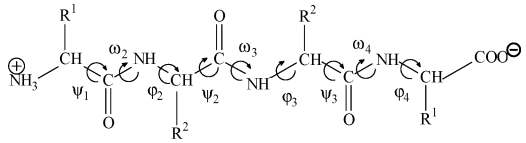

I	II
$R^1 = CH_3$	$R^1 = CD_3$
$R^2 = CD_3$	$R^2 = CH_3$

Figure 1. Tetraalanine, with the dihedral angles φ, ψ, ω indicated by arrows.

angles, namely, PPII/PPII, α helix/α helix, PPII/α helix, and α helix/PPII, give rise to the conformers considered.

The starting models were constructed assigning the values reported in Table 1 in parentheses to the φ, ψ, ω backbone dihedral angles and were optimized to obtain more reliable structures using a multistep procedure. To take into account the aqueous environment and hydrogen-bonded water molecules, each conformation was surrounded by a water solvent shell 5 Å thick with the program InsightII/Discover[34] and the positions of solvent molecules were optimized using the CVFF force field[35] while freezing the solute coordinates. Different solvent configurations were examined, and the lowest energy conformations, where the solute had the highest number of hydrogen bonded water molecules, were selected. Subsequently, quantum mechanical calculations were performed with the Gaussian 03 computational code[36] using the Becke three-parameter Lee−Yang−Parr functional (B3LYP)[37] and the 6-31G* basis set[38] on reduced systems obtained from the previous ones after deletion of the water molecules which did not form hydrogen bonds with the peptide atoms. A total of 14 water molecules were considered for each conformer. Each carbonyl oxygen had two hydrogen bonded water molecules, each amide hydrogen had one H-bonded water molecule, and both terminal groups were coordinated by three water molecules. Solvent effects were introduced through both discrete solute−solvent clusters and a continuum approach using the integral equation formalism (IEF)[39] version of the polarizable continuum model (PCM).[40] In the continuum method, the solvent is modeled by a continuum, characterized by a dielectric constant, in which a cavity contains the solute. In our models the solute consisted of the tetraalanine peptide plus 14 explicit water molecules. This choice provides at the same time a macroscopic description of the solvent and short-range solute solvent interactions such as hydrogen bonding. The selected clusters were then optimized using different stages of constraints: first, the backbone angles were frozen together with the hydrogen bonding distances (1.8 Å) of the water molecules; second, the hydrogen bonding distance constraints were released. Finally, the full geometry of the clusters was optimized allowing the backbone torsional degrees of freedom to relax. The final values are compared in Table 1 to the initial ones for the four conformers. The changes in the torsion angles ψ_1, (φ_2, ψ_2), φ_3, ω_2, and ω_3 are very limited with deviations from the starting values smaller than 13°, while major adjustments are observed for ψ_3 and ω_4 where the deviation can assume values larger than 16°. All the hydrogen bonds (15 in all) formed by peptide groups with water molecules were maintained after optimization in structure **1**, **3**, and **4**, whereas in **2** their number is slightly reduced (12 instead of 15). The values of the free energy gap of each geometry with respect to the minimum energy conformer (**1**) are also reported in Table 1. As can be seen, the PPII/PPII structure turns out to be 5.79 kcal/mol more stable than the α helix/α helix type, whereas the energy gap is smaller for the other mixed conformations which are, however, less stable than the PPII/PPII structure. The clusters after geometry optimization are shown in Figure 2.

4.2. ^{1}H NMR in the Isotropic Phase. The ^{1}H isotropic spectrum of **I** in CsPFO/D_2O at 309 K is shown in Figure 3 (trace a). The doublets due to the protonated methyl groups of the alanyl residues on the extremes of the chain at 1.66 and 1.47 ppm are present. The values of $^3J_{H^\alpha H^{Me}}$ couplings are 7.3 and 6.9 Hz, respectively for the two signals, also confirmed by the 2D J spectrum (not shown). Two singlets due to the H^α's of the two internal residues overlap at 4.43 ppm. The H^α's of the external residues appear as partially overlapped quartets centered at 4.30 and at 4.23 ppm. Because the H^N protons readily exchange with D_2O, they are not observed in the ^{1}H spectrum.

The ^{1}H isotropic spectrum of **II** in CsPFO/D_2O at the same temperature (Figure 3, trace b) shows the doublets due to the protonated methyl groups of the second and third alanyl residue. These signals are both centered at 1.53 ppm and characterized by a $^3J_{H^\alpha H^{Me}}$ of 7.1 Hz. The H^α's of the two internal residues appear here, of course, as singlets, while those of the two external ones appear as broad quartets.

The assignment of the different signals, reported in Table 2, was made on the basis of DQF COSY and NOESY experiments performed on fully protonated tetraalanine, which shows similar chemical shifts and $^3J_{H^\alpha H^{Me}}$ in CsPFO/D_2O at the same temperature.[41]

4.3. ^{1}H NMR in the Anisotropic Phase and Estimation of the Direct Couplings. The methyl portions of the ^{1}H spectra of **I** and **II** in CsPFO/D_2O in the anisotropic phase at 308 K are shown, as an example, in Figures 4 and 5 (trace a), respectively. The narrow signal at 2.1 ppm is an impurity which was also observed in the isotropic phase. At this temperature the quadrupolar splittings of water in the two samples differ by less than 2% and therefore the same degree of order can be assumed. No significant differences were found between the spectra recorded with and without ^{2}H decoupling, which indicates that ^{1}H−^{2}H dipolar couplings are negligible for the methyl protons.

TABLE 1: φ, ψ, ω Dihedral Angles in Degrees, Optimized Following the Procedure Outlined in the Text, and Related Solvation Free Energy Difference $\Delta\Delta G$ in kcal/mol with Respect to Conformer 1 of the Four Tetraalanine Structures (initial values in parentheses)

conformer	ψ_1	φ_2, ψ_2	φ_3, ψ_3	φ_4	ω_2	ω_3	ω_4	$\Delta\Delta G$
1	165.1	−57.6, 145.0	−68.8, 138.4	−78.2	166.9	175.7	158.6	0.00
	(165.0)	(−70.0, 155.0)	(−80.0, 145.0)	(−80.0)	(180.0)	(180.0)	(180.0)	
2	164.6	−84.7, −66.8	−85.4, −32.5	−83.0	−179.2	−177.8	167.3	5.79
	(165.0)	(−80.0, −60.0)	(−80.0, −60.0)	(−80.0)	(180.0)	(180.0)	(180.0)	
3	176.0	−73.0, 168.0	−76.3, −76.2	−88.1	173.9	177.9	168.9	3.58
	(165.0)	(−80.0, 165.0)	(−80.0, −60.0)	(−80.0)	(180.0)	(180.0)	(180.0)	
4	164.4	−79.3, −59.2	−81.3, 163.4	−74.9	−179.5	171.5	161.3	2.36
	(165.0)	(−80.0, −60.0)	(−80.0, 165.0)	(−80.0)	(180.0)	(180.0)	(180.0)	

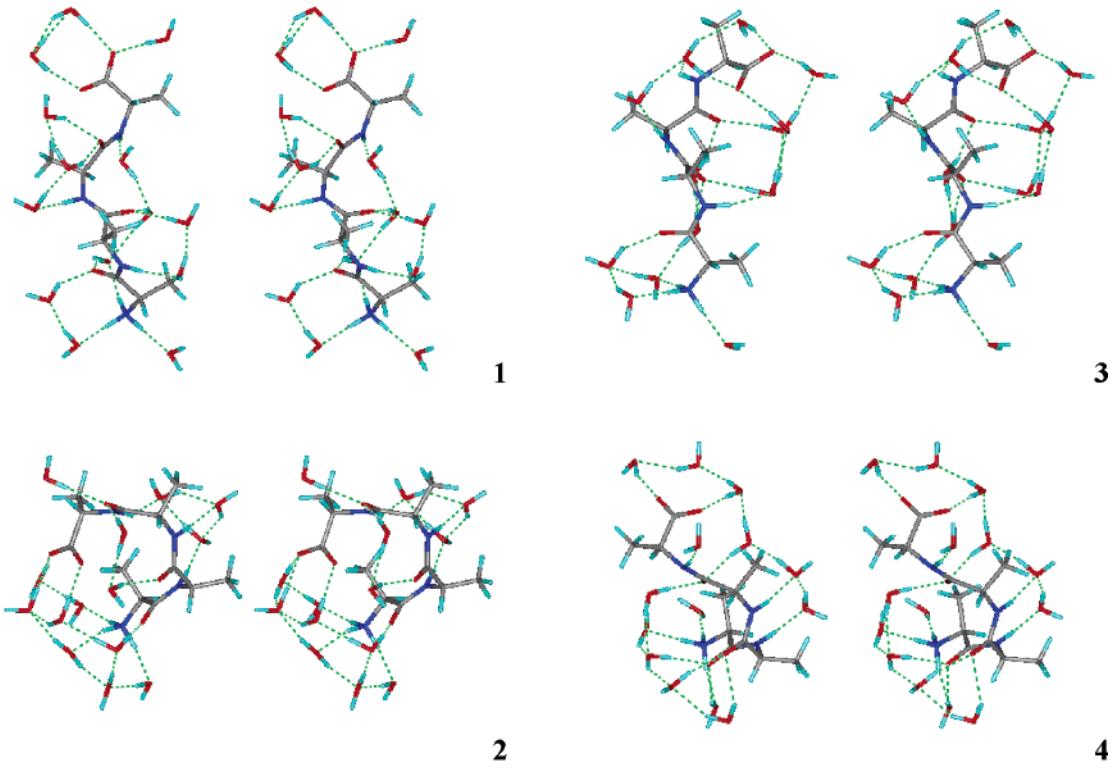

Figure 2. Stereoviews of the four tetraalanine conformers obtained after the multistep optimization.

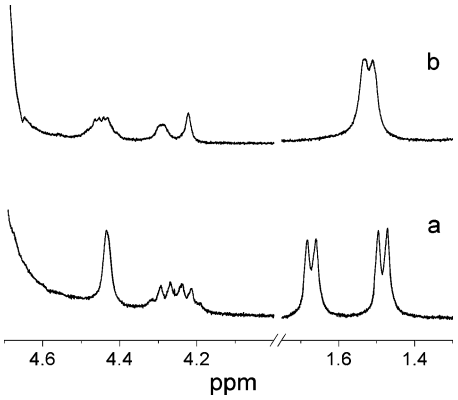

Figure 3. ^{1}H spectrum of **I** (trace a) and of **II** (trace b) in CsPFO/D_2O in the isotropic phase at 309 K.

TABLE 2: ^{1}H Chemical Shift Assignment in the Molecules I and II

^{1}H chemical shift (ppm)[a]	assignment[b]	^{1}H chemical shift (ppm)[a]	assignment[b]
1.66	H^{Me1}	4.23	$H^{\alpha 1}$
1.53	H^{Me2}	4.43	$H^{\alpha 2}$
1.53	H^{Me3}	4.43	$H^{\alpha 3}$
1.47	H^{Me4}	4.30	$H^{\alpha 4}$

[a] The proton chemical shifts are referenced to the water signal, which was set at 4.75 ppm. [b] The alanyl residues are numbered starting from the N-terminus.

Since in the anisotropic phase the intense water signal is partially overlapped to that of the methine protons, we focused on the methyl region for our analysis. On the basis of distance considerations, the spectrum is expected to be dominated by the dipolar interaction among the protons of each methyl group ($D(H^{Mei})$) and between the proton of a methine and those of the methyl in the same *i* residue ($D(H^{\alpha i}, H^{Mei})$). If the methyl

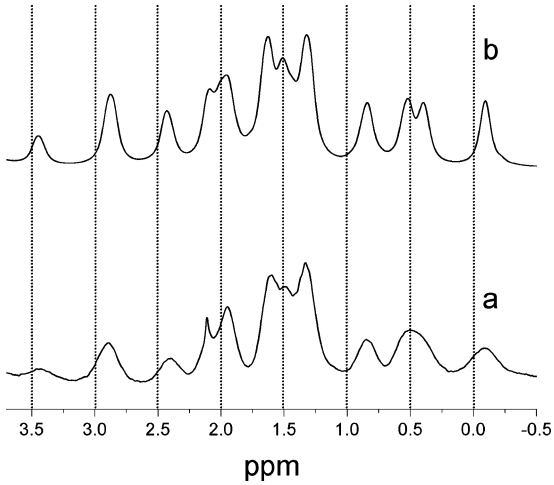

Figure 4. Experimental (a) and simulated (b) ^{1}H spectrum of **I** in CsPFO/D_2O in the anisotropic phase at 308 K. Vertical lines are drawn to help in the comparison between the two spectra.

is assumed to rotate fast about its C_3 axis, the pattern expected for each methyl is a triplet due to the intramethyl interaction, each peak being further split in a doublet by the methyl−methine proton dipolar interaction.

The comparison of the spectra of each sample recorded at different temperatures in the anisotropic phase allowed the patterns expected for the two alanyl residues in each molecule to be identified. For sample **I**, in which the two fully protonated residues differ in chemical shift, the attribution of the patterns was confirmed by 2D J-resolved spectroscopy at 308 K. A series of spectra recorded for this sample at different temperatures is shown in Figure 6 as an example. The patterns due to the two methyl groups are highlighted in the upper trace.

In **II** the two patterns were identified on the basis of the structure of the central feature and of the relative integrals of

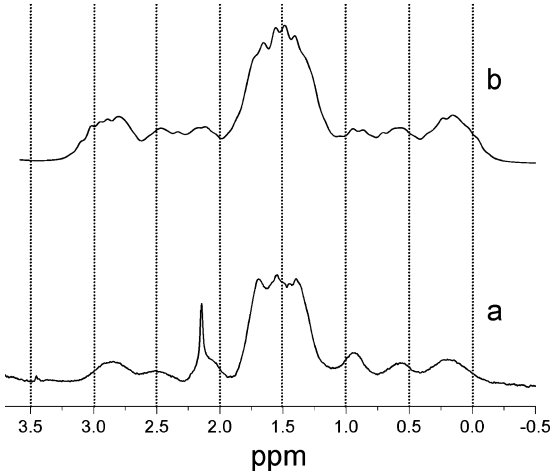

Figure 5. Experimental (a) and simulated (b) ^{1}H spectrum of **II** in CsPFO/D_2O in the anisotropic phase at 308 K. Vertical lines are drawn to help in the comparison between the two spectra.

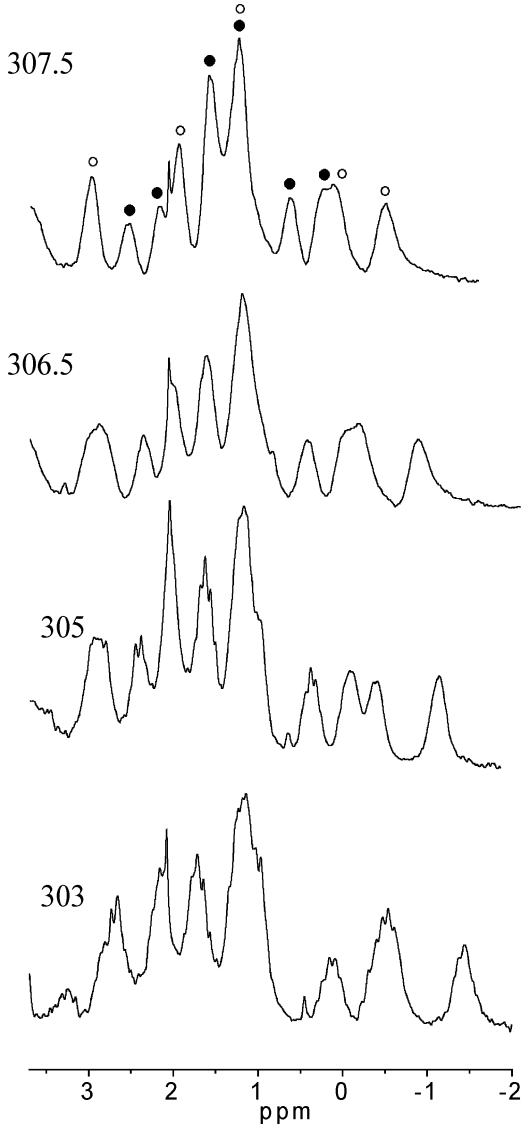

Figure 6. ^{1}H spectra of **I** in CsPFO/D_2O in the anisotropic phase at different temperatures. In the upper trace, the patterns due to the first (○) and last (●) methyl group of the chain are highlighted.

the lines flanking the central signal. In fact, the integrals of the most external peaks are approximately double with respect to those of the internal ones and the only feasible assignment predicts a $D(H^{\alpha i}, H^{Mei}) = 0$ for one residue.

TABLE 3: Estimated Values of Dipolar Couplings in I and II in the Anisotropic Phase and Parameters Used in the Simulations of the ^{1}H Spectra[a]

	estimated value[b] from **I**	estimated value[b] from **II**	value used in the simulation
$D(H^{\alpha 1},H^{Me1})$	80		−85
$D(H^{\alpha 2},H^{Me2})$		0	−4
$D(H^{\alpha 3},H^{Me3})$		48	48
$D(H^{\alpha 4},H^{Me4})$	52		48
$D(H^{Me1})$	156		156
$D(H^{Me2})$		134	−136
$D(H^{Me3})$		76	78
$D(H^{Me4})$	79		−79
$D(H^{\alpha 1},H^{\alpha 2})$			32
$D(H^{\alpha 1},H^{\alpha 3})$			−4
$D(H^{\alpha 1},H^{\alpha 4})$			−1
$D(H^{\alpha 1},H^{Me2})$			31
$D(H^{\alpha 1},H^{Me3})$			0
$D(H^{\alpha 1},H^{Me4})$			−2
$D(H^{Me1},H^{\alpha 2})$			7
$D(H^{Me1},H^{\alpha 3})$			2
$D(H^{Me1},H^{\alpha 4})$			4
$D(H^{Me1},H^{Me4})$			−1
$D(H^{Me2},H^{Me3})$			−12
$D(H^{\alpha 2},H^{\alpha 3})$			−33
$D(H^{\alpha 2},H^{\alpha 4})$			−6
$D(H^{\alpha 2},H^{Me3})$			−19
$D(H^{\alpha 2},H^{Me4})$			−4
$D(H^{Me2},H^{\alpha 3})$			−11
$D(H^{Me2},H^{\alpha 4})$			−12
$D(H^{\alpha 3},H^{\alpha 4})$			2
$D(H^{\alpha 3},H^{Me4})$			-9
$D(H^{Me3},H^{\alpha 4})$			-12
cs (H^{Me1})			1.70
cs (H^{Me2})			1.53
cs (H^{Me3})			1.53
cs (H^{Me4})			1.48
cs ($H^{\alpha 1}$)			4.23
cs ($H^{\alpha 2}$)			4.43
cs ($H^{\alpha 3}$)			4.43
cs ($H^{\alpha 4}$)			4.30
$J(H^{\alpha 1}, H^{Me1})$			7.3
$J(H^{\alpha 2}, H^{Me2})$			7.1
$J(H^{\alpha 3}, H^{Me3})$			7.1
$J(H^{\alpha 4}, H^{Me4})$			6.9

[a] The dipolar and the scalar couplings are given in Hz, while the chemical shifts in ppm. [b] Only absolute values could be determined (see text).

The spectra allowed only the strongest dipolar couplings to be estimated, with no indication of the relative signs. The oriented spectra were fitted with the SpinWorks program. The program calculates the NMR transition frequencies and intensities for the partially ordered spin system from estimates of chemical shifts, J couplings, and dipolar couplings of the magnetically active nuclei. These parameters were at first manually adjusted until sufficient resemblance between the experimental and calculated spectra was obtained; then the direct couplings and shifts were optimized through an automated least-squares routine minimizing the deviation between calculated and experimental frequencies. The $^3J_{H\alpha H^{Me}}$ couplings between the methyl protons and the α proton of the same alanyl residue were assumed to be identical to the values found in the isotropic phase, the anisotropic part of this interaction being neglected. The sign of $^3J_{H\alpha H^{Me}}$ was taken from the literature.[42] Additional J couplings extending over five or six bonds were neglected.

The estimated absolute values of $D(H^{Mei})$ and $D(H^{\alpha i}, H^{Mei})$ for each residue are given in Table 3 for the two isotopomers at 308 K. Only small variations (∼0.1 ppm) were observed for

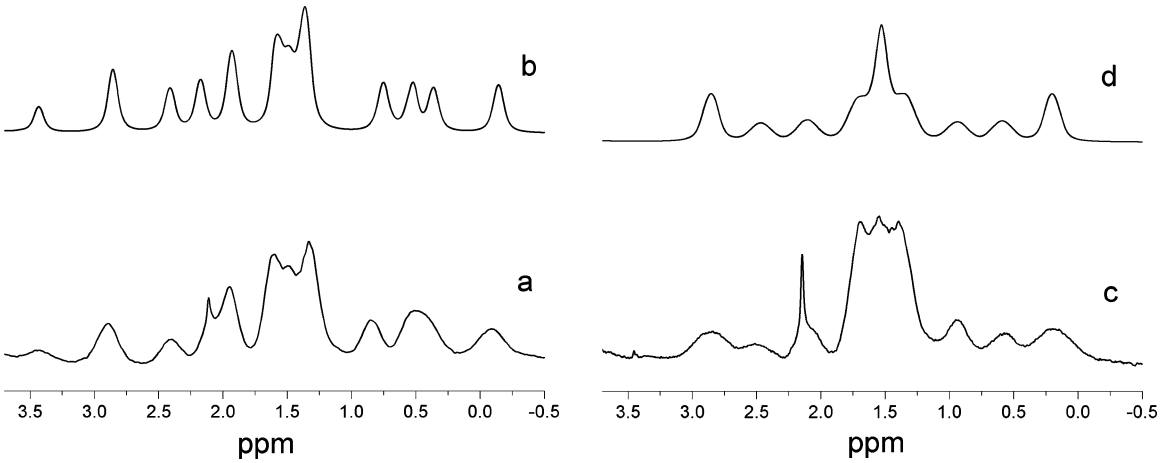

Figure 7. Experimental ^{1}H spectra of **I** (trace a) and **II** (trace c) in CsPFO/D_2O in the anisotropic phase at 308 K compared to the poorly simulated spectra shown in b and d obtained using the best fitting parameters derived for conformer **3**.

the chemical shift in the anisotropic with respect to the isotropic phase. This indicates negligible values of the proton chemical shift anisotropy, as usually found.[24]

4.4. Conformers and Orientations. 4.4.1. Strategy. The set of $D(H^{Mei})$ and $D(H^{\alpha i}, H^{Mei})$ absolute values obtained from the fitting of the spectra could be used in eq 1 in order to obtain the best combination of signs compatible with a given geometry, assuming the presence of a single rigid conformer. The best combination was chosen among all the possible ones as that giving the smallest variance in the fitting. This combination is associated, in turn, to the best order matrix.

In the calculations, the molecular frame was set in the PAS of the inertial tensor for each conformer, with the *z* axis chosen as the one with the smallest value of the inertial moment. Moreover, the free rotation of each methyl group about its C_3 symmetry axis was assumed. In fact, the value of $D(H^{Mei})$ was calculated as the average of the couplings between the three couples of methyl protons and, analogously, $D(H^{\alpha i}, H^{Mei})$ was the average of the couplings between H^α and each one of the three protons of the methyl group. In addition, since the chemical shifts of the internal methyl groups overlap, we tested both possible attributions of the two patterns identified in the spectrum of **II**, performing the fitting with both possible pattern combinations.

The strategy outlined was checked a posteriori by calculating the spectra of the isotopomers **I** and **II** using the dipolar couplings between *all* the protons derived from the values of the elements of the order matrix resulting from the best fit.

4.4.2. Determination of Preferred Conformation and Simulation of the Spectra. The minimum variance was obtained for conformer **1**, the variance being in this case at least 10 times smaller than those for the other three conformers considered. However, comparison between the spectrum calculated using the best set of order parameters and the experimental one revealed that the two dipolar couplings $D(H^{Me1},H^{\alpha 2})$ and $D(H^{\alpha 3},H^{Me4})$ were slightly overestimated (15 vs 7 Hz and -17 vs -9 Hz, respectively). This fact might suggest that the molecular extremes are not well described by a single dihedral angle due to a certain degree of flexibility. For the N-terminus, this hypothesis is consistent with the results of a theoretical study on tetraalanine cation, where a relatively broad probability distribution of the dihedral angle ψ_1 was derived using molecular dynamics simulations.[33] In particular, conformers with ψ_1 ranging from 140 to $-140°$ are significantly populated. In our case, if the values of the order elements are fixed to those reported in Table 4 (see below), the value of the coupling $D(H^{Me1},H^{\alpha 2})$ for conformers with ψ_1 ranging from -160 to $-120°$ is about 10 Hz, which is significantly smaller than the value of 15 Hz, calculated for $\psi_1 = 165°$.

TABLE 4: Order Parameters and Principal Axes Order Parameters

S_{xx}	−0.011	$S_{x'x'}$	0.025
S_{yy}	0.009	$S_{y'y'}$	0.015
S_{zz}	0.002	$S_{z'z'}$	−0.040
S_{xy}	−0.015		
S_{xz}	−0.025		
S_{yz}	−0.017		

As far as φ_4 is concerned, if it is assumed that conformers with φ_4 in the region between -180 and $-100°$ are populated, as has been predicted for the anionic and zwitterionic forms of tetraalanine,[33] the absolute coupling $D(H^{\alpha 3},H^{Me4})$ decreases, as required by the spectral simulation.

The spectra calculated for conformer **I** using the parameters reported in Table 3 are shown in Figures 4 and 5 (trace b).

To compare the quality of the simulation for different conformers, Figure 7 shows an example of poorly simulated spectra calculated using the best fitting parameters derived for conformer **3**, for which the minimum variance is 10 times larger than that of **1**. In this case, the spectrum of isotopomer **I** poorly reproduces the positions of the peaks in the pattern due to the last methyl of the chain as $D(H^{\alpha 4},H^{Me_4})$ is sensibly underestimated, whereas in isotopomer **II** the simulated central feature is remarkably different from the experimental one.

From these results, conformer **1** can be safely indicated as the most populated one and significant contributions from other conformers can be excluded. This is in agreement with the results obtained on cationic tetraalanine in water by polarized Raman, Fourier transform IR, and vibrational CD techniques,[22] as well as with experimental findings on other alanine-based oligopeptides in water.

4.4.3. Full Order Parameters. Table 4 lists the set of order parameters in the molecular inertial frame derived from the fitting procedure and their values.

The order of magnitude of the order parameters is comparable to that already observed for similar systems.[15,43] According to a classification already proposed for some amides in CsPFO/D_2O,[44] our molecule would be a moderate/strong orienter, as the root-mean-square of the three eigenvalues of the order matrix is 0.028. A rough estimate of the possible values for the peptide order parameters[43] yields the limiting values of $+0.06$ for perfect orientation normal to the micelle surface and -0.03 for perfect orientation in the plane of the surface, within the assumptions

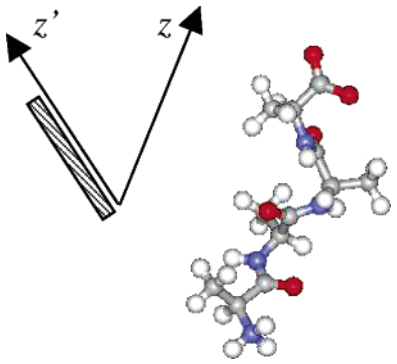

Figure 8. Orientation of the z (associated to the molecular inertial PAS) and z' (associated to the order PAS) axes and structure of tetraalanine dissolved in CsPFO. The situation in which z' axis lies in the disk plane, represented by the rectangle, is depicted.

that the peptide partitions without preference between the micelle−water interface and the bulk water, and does not reside in the micelle itself, that the micelle order parameter is about 0.3 (as measured for the nematic phase of CsPFO/water at ∼40 wt % and $T - T_{NI} = 1$ °C[45]), and that the interfacial thickness is 10 Å. For the calculations, micelle dimensions reported in the literature were assumed.[46] The value of $S_{z'z'}$ found by us is more negative than the minimum allowed according to this model, which might suggest that tetraalanine preferentially resides in the interface.

The negative sign of the major order parameter $S_{z'z'}$ indicates that the molecule is on average oriented with the principal axis of the order PAS z' making an angle larger than the magic angle with the normal axis of the CsPFO disks, which is parallel to the external magnetic field. Moreover, the relatively high absolute value of $S_{z'z'}$ suggests that z' is almost parallel to the disk surface. The Euler angles α,β,γ determining the relative orientation of the PAS of the inertial tensor and that of the order matrix are 30, 54, and 200°, respectively. The long axis of the molecule is then tilted with respect to z' by 54° (Figure 8), hence closer to the normal of the CsPFO disks. The molecule results tilted with respect to the micelle surface, and this is probably related to the charge difference between the extremes of the molecule; whereas the positively charged N-terminus is expected to be attracted by the negatively charged disk surface, the negatively charged C-terminus points away from it.

5. Conclusions

In this study the interpretation of NMR data together with theoretical calculations of molecular geometry allowed us to obtain information on the conformation and orientation of a peptide in a partially ordered system. In particular, the conformation of tetraalanine in CsPFO/D_2O could be determined from the nonvanishing dipolar couplings due to the anisotropic medium. The experimental data resulted to be compatible with the presence of a single PPII type conformer, in agreement with the findings for other alanine-based oligopeptides. The comparison of our results with those reported in the literature concerning the conformation of cationic tetraalanine in water[22] suggests that neither the protonation state nor the interaction of the oligopeptide with the hydrophobic species of the mesophase induces conformational changes with respect to the pure water phase. In addition, our data are compatible with a certain degree of flexibility of the molecular extremes.

In the nematic phase of the CsPFO/D_2O system, tetraalanine tends to orient with the major axis of the order matrix tilted with respect to the phase director by more than the magic angle and almost parallel to the micelle surface, with the positively charged N-terminus probably lying on the surface of the micelle while the rest of the molecule is tilted away. We speculated that this orientation might be related to the protonation state of the molecule. A study of the orientation of molecules differing in the protonation state could help in testing this hypothesis. Moreover, the collection of additional residual couplings for the molecule here investigated, for example using ^{13}C isotopomers, might provide a further test on conformational diversity.

Acknowledgment. We wish to thank Shimon Vega for providing the deuterated samples and for helpful comments. S.P. wishes to thank the Italian National Research Council for financial support (Grant No. 201.22-03).

References and Notes

(1) Tandford, C. *Adv. Protein Chem.* **1968**, *23*, 121−282.
(2) Dill, K. A. *Protein Sci.* **1999**, *8*, 1166−1180.
(3) Gnanakaran, S.; Garcia, A. E. *J. Phys. Chem. B* **2003**, *107*, 12555−12557.
(4) Tiffany, M. L.; Krimm, S. *Biopolymers* **1968**, *6*, 1379−1382.
(5) Rippon, W. B.; Walton, A. G. *Biopolymers* **1971**, *10*, 1207−1212.
(6) Drake, A. F.; Siligardi, G.; Gibbons, W. A. *Biophys. Chem.* **1988**, *31*, 143−146.
(7) Park, S. H.; Shalongo, W.; Stellwagen, E. *Protein Sci.* **1997**, *6*, 1694−1700.
(8) Woody, R. W. *Adv. Biophys. Chem.* **1992**, *2*, 37−79.
(9) Sreerama, N.; Woody, R. W. *Biochemistry* **1994**, *33*, 10022−10025.
(10) Tiffany, M. L.; Krimm, S. *Biopolymers* **1968**, *6*, 1767−1770.
(11) Keiderling, T. A.; Silva, R. A.; Yoder, G.; Dukor, R. K. *Bioorg. Med. Chem.* **1999**, *7*, 133−141.
(12) Blanch, E. W.; Morozova-Roche, L. A.; Cochran, D. A.; Doig, A. J.; Hecht, L.; Barron, L. D. *J. Mol. Biol.* **2000**, *301*, 553−563.
(13) Shi, Z.; Olson, C.; Rose, G.; Baldwin, R.; Kallenbach, N. *Proc. Natl. Acad. Sci. U.S.A.* **2002**, *99*, 9190−9195.
(14) Poon, C. D.; Samulski, E. T.; Weise, C. F.; Weisshaar, J. C. *J. Am. Chem. Soc.* **2000**, *122*, 5642−5643.
(15) Weise, C. F.; Weisshaar, J. C. *J. Phys. Chem. B* **2003**, *107*, 3265−3277.
(16) Kim, Y. S.; Wang, J.; Hochstrasser, R. M. *J. Phys. Chem. B* **2005**, *109*, 7511−7521.
(17) Han, W. G.; Jalkanen, K. J.; Elstner, M.; Suhai, S. *J. Phys. Chem. B* **1998**, *102*, 2587−2602.
(18) Woutersen, S.; Hamm, P. *J. Phys. Chem. B* **2000**, *104*, 11316−11320.
(19) Woutersen, S.; Hamm, P. *J. Chem. Phys.* **2001**, *114*, 2727−2737.
(20) Schweitzer-Stenner, R.; Eker, F.; Huang, Q.; Griebenow, K. *J. Am. Chem. Soc.* **2001**, *123*, 9628−9633.
(21) Eker, F.; Griebenow, K.; Schweitzer-Stenner, R. *J. Am. Chem. Soc.* **2003**, *125*, 8178−8185.
(22) Schweitzer-Stenner, R.; Eker, F.; Griebenow, K.; Cao, X.; Nafie, L. A. *J. Am. Chem. Soc.* **2004**, *126*, 2768−2776.
(23) Shi, Z.; Woody, R. W.; Kallenbach, N. R. *Adv. Protein Chem.* **2002**, *62*, 163−240.
(24) Emsley, J. N.; Lindon, J. C. *NMR Spectroscopy Using Liquid Crystal Solvents*; Pergamon Press: Oxford, U.K., 1975.
(25) Prestegard, J. H.; Al-Hashimi, H. M.; Tolman, R. J. *Q. Rev. Biophys.* **2000**, *33*, 371−424.
(26) Boden, N.; Corne, S. A.; Jolley, K. W. *J. Phys. Chem.* **1987**, *91*, 4092−4105.
(27) Kimura, A.; Kuni, N.; Fujiwara, H. *J. Am. Chem. Soc.* **1997**, *119*, 4719−4725.
(28) Kimura, A.; Takamoto, K.; Fujiwara, H. *J. Am. Chem. Soc.* **1998**, *120*, 9656−9661.
(29) Pizzanelli, S.; Kababya, S.; Frydman, V.; Landau, M.; Vega, S. *J. Phys. Chem. B* **2005**, *109*, 8029−8039.
(30) Marat, K. SpinWorks; University of Manitoba, Winnipeg, Manitoba, Canada. http://www.umanitoba.ca/chemistry/nmr/spinworks/.
(31) Trademark of Wolfram Research Inc.
(32) Diehl, P. Molecular Structure from Dipolar Couplings In *Nuclear Magnetic Resonance of Liquid Crystals*; Emsley, J. W., Ed.; Reidel: Dordrecht, 1985; pp 147−148.
(33) Blatt, H. D.; Smith, P. E.; Pettitt, B. M. *J. Phys. Chem. B* **1997**, *101*, 7628−7634.
(34) InsightII/Discover 2.9 MSI/Accelrys, San Diego, CA 92121.

(35) Dauber-Osguthorpe, P.; Roberts, V. A.; Osguthorpe, D. J.; Wolff, J.; Genest, M.; Hagler, A. T. *Proteins*: *Struct., Funct., Genet.* **1988**, *4*, 31−47.

(36) Frisch, M. J.; Trucks, G. W.; Schlegel, H. B.; Scuseria, G. E.; Robb, M. A.; Cheeseman, J. R.; Montgomery, J. A., Jr.; Vreven, T.; Kudin, K. N.; Burant, J. C.; Millam, J. M.; Iyengar, S. S.; Tomasi, J.; Barone, V.; Mennucci, B.; Cossi, M.; Scalmani, G.; Rega, N.; Petersson, G. A.; Nakatsuji, H.; Hada, M.; Ehara, M.; Toyota, K.; Fukuda, R.; Hasegawa, J.; Ishida, M.; Nakajima, T.; Honda, Y.; Kitao, O.; Nakai, H.; Klene, M.; Li, X.; Knox, J. E.; Hratchian, H. P.; Cross, J. B.; Adamo, C.; Jaramillo, J.; Gomperts, R.; Stratmann, R. E.; Yazyev, O.; Austin, A. J.; Cammi, R.; Pomelli, C.; Ochterski, J. W.; Ayala, P. Y.; Morokuma, K.; Voth, G. A.; Salvador, P.; Dannenberg, J. J.; Zakrzewski, V. G.; Dapprich, S.; Daniels, A. D.; Strain, M. C.; Farkas, O.; Malick, D. K.; Rabuck, A. D.; Raghavachari, K.; Foresman, J. B.; Ortiz, J. V.; Cui, Q.; Baboul, A. G.; Clifford, S.; Cioslowski, J.; Stefanov, B. B.; Liu, G.; Liashenko, A.; Piskorz, P.; Komaromi, I.; Martin, R. L.; Fox, D. J.; Keith, T.; Al-Laham, M. A.; Peng, C. Y.; Nanayakkara, A.; Challacombe, M.; Gill, P. M. W.; Johnson, B.; Chen, W.; Wong, M. W.; Gonzalez, C.; Pople, J. A. *Gaussian 03, Revision A.1*; Gaussian, Inc.: Pittsburgh, PA, 2003.

(37) (a) Becke, A. D. *J. Chem. Phys.* **1993**, *98*, 5648−5652. (b) Lee, C.; Yang, W.; Parr, R. G. *Phys. Rev. B* **1988**, *37*, 785−789.

(38) (a) Ditchfield, R.; Hehre, W. J.; Pople, J. A. *J. Chem. Phys.* **1971**, *54*, 724−728. (b) Hehre, W. J.; Ditchfield, R.; Pople J. A. *J. Chem. Phys.* **1972**, *56*, 2257−2269. (c) Dill, J. D.; Pople, J. A. *J. Chem. Phys*. **1975**, *62*, 2921−2923.

(39) (a) Cancès, E.; Mennucci, B. *J. Math. Chem.* **1998**, *23*, 309−326. (b) Cancès, E.; Mennucci, B.; Tomasi, J. *J. Chem. Phys.* **1997**, *107*, 3032−3041. (c) Mennucci, B.; Cancès, E.; Tomasi, J. *J. Phys. Chem. B* **1997**, *101*, 10506−10517.

(40) (a) Miertus, S.; Scrocco, E.; Tomasi, J. *Chem. Phys.* **1981**, *55*, 117−129. (b) Cammi, R.; Tomasi, J. *J. Comput. Chem.* **1995**, *16*, 1449−1458.

(41) Work in progress.

(42) Madison, V.; Kopple, K. D. *J. Am. Chem. Soc.* **1980**, *102*, 4855−4863.

(43) Weise, C. F.; Weisshaar, J. C. *J. Phys. Chem. B* **2003**, *107*, 6552−6564.

(44) Johannesson, H.; Furo, I.; Halle, B. *Phys. Rev. E* **1996**, *53*, 4904−4917.

(45) Jolley, K. W.; Boden, N.; Parker, D.; Henderson, J. R. *Phys. Rev. E* **2002**, *65*, 041713.

(46) Holmes, M. C.; Reynolds, D. J.; Boden, N. *J. Phys. Chem.* **1987**, *91*, 5257−5262.